

Dimerization of the Klenow Fragment of *Escherichia coli* DNA Polymerase I Is Linked to Its Mode of DNA Binding[†]

Michael F. Bailey,[‡] Edwin J. C. Van der Schans, and David P. Millar*

Department of Molecular Biology, The Scripps Research Institute, 10550 North Torrey Pines Road, La Jolla, California 92037

Received November 21, 2006; Revised Manuscript Received March 28, 2007

ABSTRACT: Upon associating with a proofreading polymerase, the nascent 3′ end of a DNA primer/template has two possible fates. Depending upon its suitability as a substrate for template-directed extension or postsynthetic repair, it will bind either to the 5′–3′ polymerase active site, yielding a polymerizing complex, or to the 3′–5′ exonuclease site, yielding an editing complex. In this investigation, we use a combination of biochemical and biophysical techniques to probe the stoichiometry, thermodynamic, and kinetic stability of the polymerizing and editing complexes. We use the Klenow fragment of *Escherichia coli* DNA polymerase I (KF) as a model proofreading polymerase and oligodeoxyribonucleotide primer/templates as model DNA substrates. Polymerizing complexes are produced by mixing KF with correctly base paired (matched) primer/templates, whereas editing complexes are produced by mixing KF with multiply mismatched primer/templates. Electrophoretic mobility shift titrations carried out with matched and multiply mismatched primer/templates give rise to markedly different electrophoretic patterns. In the case of the matched primer/template, the KF·DNA complex is represented by a slow moving band. However, in the case of the multiply mismatched primer/template, the complex is predominantly represented by a fast moving band. Analytical ultracentrifugation measurements indicate that the fast and slow moving bands correspond to 1:1 and 2:1 KF·DNA complexes, respectively. Fluorescence anisotropy titrations reveal that KF binds with a higher degree of cooperativity to the matched primer/template. Taken together, these results indicate that KF is able to dimerize on a DNA primer/template and that dimerization is favored when the first molecule is bound in the polymerizing mode, but disfavored when it is bound in the editing mode. We suggest that self-association of the polymerase may play an important and as yet unexplored role in coordinating high-fidelity DNA replication.

Since it was first described in the late 1960s (1), the Klenow fragment of *Escherichia coli* DNA polymerase I (KF)¹ has served as the flagship for the study of proofreading polymerase function. Its tractability as a model stems from the fact that it contains both 5′–3′ polymerase and 3′–5′ exonuclease (editing) activities within the same polypeptide chain, can carry out high-fidelity DNA synthesis without the need for accessory factors, and can be produced using standard recombinant techniques in quantities sufficient for biochemical, biophysical, and structural studies. Consequently, a significant body of data is available for this enzyme, providing an ideal framework for mechanistic studies of high-fidelity template-directed DNA synthesis. Importantly, KF shares structural (2–6) and mechanistic (7–11) features with DNA polymerases from several different

families; hence, insights gleaned from studies of KF are likely to be generally applicable to a wide variety of DNA polymerases.

Structural and biochemical studies have shown that the polymerase and 3′–5′ exonuclease activities are located in separate structural domains of KF (12–15). The polymerase domain resembles a half-open right hand, with fingers, palm, and thumb subdomains (2), each of which plays an important role in the polymerization reaction. The fingers position the template strand and bind the incoming deoxynucleotide substrate; the palm orients the nascent primer strand in readiness for phosphodiester bond formation, and the thumb binds the resulting duplex DNA product. The 3′–5′ exonuclease domain contains a binding site for single-stranded DNA and a cluster of highly conserved acidic residues that bind the catalytic metal ions required for phosphodiester bond hydrolysis (12, 16).

Because of the physical separation of the polymerase (pol) and 3′–5′ exonuclease (exo) active sites, a DNA primer/template must interact with KF in different ways during a polymerization or editing reaction. The structural details of the polymerizing complex are not available directly, because a cocrystal structure of KF with DNA bound to the pol site is not available. However, such structures have been determined for the KF homologues encoded by *Thermus aquaticus* and bacteriophage T7 (17, 18). These structures

[†] This work was supported by a grant to D.P.M. from the National Institute of General Medical Sciences (GM 44060). M.F.B. is the recipient of C. J. Martin Fellowship 145843 from the Australian National Health and Medical Research Council.

* To whom correspondence should be addressed. Telephone: (858) 784-9870. Fax: (858) 784-9067. E-mail: millar@scripps.edu.

[‡] Current address: Department of Biochemistry and Molecular Biology, The Bio21 Molecular Science and Biotechnology Institute, The University of Melbourne, 30 Flemington Rd., Parkville, Victoria 3010, Australia.

¹ Abbreviations: KF, Klenow fragment of *E. coli* DNA polymerase I; pol site, 3′–5′ polymerase active site; exo site, 3′–5′ exonuclease active site.

Table 1: Sequences, Details, and Nomenclature of Primer/Template Duplexes Used in This Study

Primer/template nucleotide sequence ^{a,b}	No. of mismatches	Duplex name
5'-TCGCAGCCGTCAAAATG-3' 3'-AGCGTCGGCAGTTTACATATAGCCGA-5'	0	F17/27-0
5'-TCGCAGCCGTCAA ^{AATG} -3' 3'-AGCGTCGGCAGTT _{CCTT} ATATAGCCGA-5'	4	F17/27-4
5'-TCGAGTCGCAGCCGTCAAAATG-3' 3'-AGCTCAGCGTCGGCAGTTTACATATAGCCGA-5'	0	F22/32-0
5'-TCGAGTCGCAGCCGTCAA ^{AATG} -3' 3'-AGCTCAGCGTCGGCAGTT _{CCTT} ATATAGCCGA-5'	4	F22/32-4
5'-TCGCAGCCGTCAAAATG-3' 3'-AGCGTCGGCAGTTTACATA-5'	0	F17/20-0

^a T denotes that thymidine 1 (from the 5' end of the primer strand) is labeled with fluorescein via a C₆ amino linker. ^b A mismatched base pair is highlighted by a superscripted base in the primer strand opposite a subscripted base in the template strand.

show that the primer/template duplex adopts A-form double-helical geometry close to the primer 3' terminus, which is bound in the pol site in the palm subdomain, while the duplex region upstream from the primer 3' terminus is bound by the thumb subdomain. Additionally, two cocrystal structures of KF with duplex DNA bound in an editing complex are available (16, 19). These structures reveal that the last four bases of the primer strand are bound to the exo domain in an extended single-stranded conformation, while the remainder of the primer/template duplex interacts with the thumb subdomain. However, the duplex appears to be translocated by 2–3 bp with respect to the polymerizing complex.

Time-resolved fluorescence anisotropy measurements with internally dansyl-labeled primer/templates have been used to distinguish the two binding modes of the KF•DNA complex in solution (20, 21). These studies have shown that primer/templates naturally partition between two binding modes and that the distribution varies directly with the mismatch content. As expected, correctly base paired primer/templates (i.e., containing no mismatched base pairs) bind predominantly to the pol site and thereby serve as suitable reagents for studying the polymerizing complex (20, 21). In contrast, primer/templates containing four consecutive terminal mismatches bind exclusively to the exo site and constitute ideal reagents for studying the editing complex.

The time-resolved anisotropy measurements are also sensitive to the overall size of the KF•DNA complex. We have observed that the rotational correlation time of the complex increases sigmoidally as a function of protein concentration, suggesting that multiple KF molecules can bind to a single DNA primer/template (M. F. Bailey and D. P. Millar, forthcoming manuscript). However, there has been no systematic study of this phenomenon reported to date.

In this study, we use a variety of biochemical and biophysical techniques to investigate the linkage between the DNA binding mode and the interaction stoichiometry. Our results show that KF can associate with model DNA primer/templates either as a monomer or as a dimer. Moreover, we demonstrate that the ability of KF to dimerize on DNA is linked to the primary binding mode of the enzyme (polymerizing vs editing). The functional implications of this novel finding are discussed.

MATERIALS AND METHODS

Preparation of Oligonucleotide Primer/Templates. Oligo-(deoxyribo)nucleotides representing the primer and template

strands used in this work were synthesized on a Gene Assembler (Pharmacia) using standard β -cyanoethyl phosphoramidite chemistry (Table 1). As the final step in the synthesis, Aminolink-2 (Applied Biosystems) was coupled to the 5' end of the primer strands to provide a unique site for postsynthetic derivatization with the succinimidyl ester of 5-carboxyfluorescein (Invitrogen) (22). Oligonucleotides were purified by denaturing PAGE and transferred into the experimental buffer [50 mM Tris-HCl (pH 7.5) and 3 mM MgCl₂] using size exclusion chromatography. Preparations were greater than 99% pure according to analytical reversed-phase HPLC. Oligonucleotide concentrations were determined spectrophotometrically using ϵ_{260} values calculated by the nearest-neighbor method (23). The measured 260 nm absorption of the fluorescein-labeled primers was corrected to account for the contribution of the probe. Primer/template duplexes were prepared by combining an equal volume of a 10 μ M solution of the labeled primer with a 10.5 μ M solution of the appropriate template. Mixtures were heated at 80 °C for 10 min and then allowed to cool to room temperature overnight. Primer/template duplexes are named according to (i) the length of the fluorescein-labeled primer strand, (ii) the length of the (semi)complementary template strand, and (iii) the number of mismatched base pairs. For example, the constructs used most extensively in this study are designated F17/27-0 and F17/27-4 because they each comprise a 17-nucleotide fluorescein-labeled primer strand and a 27-nucleotide template strand. F17/27-0 does not contain any mismatched base pairs, while F17/27-4 contains four consecutive mismatched base pairs located near the 3' end of the primer strand.

Preparation of the Klenow Fragment. The KF derivative used in this work contains the D424A mutation. This essentially abolishes the 3'–5' exonuclease activity but does not compromise DNA binding, enabling investigation of the protein–DNA interaction without the added complication of substrate degradation (12). Plasmid pVD2 encoding D424A KF was provided by C. Joyce (Yale University, New Haven, CT). The protein was overexpressed by heat induction in *E. coli* strain CJ376, purified by successive rounds of anion exchange and hydrophobic interaction chromatography, and transferred into the experimental buffer by size exclusion chromatography (24). Preparations were >95% pure, according to SDS–PAGE. KF concentrations were determined spectrophotometrically using an ϵ_{280} value of 5.88×10^4 M^{–1} cm^{–1}, calculated from the primary amino acid sequence using

SEDNTERP (Amgen). KF stocks (typically 50–150 μM) were aliquoted into 50 μL portions, flash-frozen in liquid nitrogen, and stored at -80°C . Working stocks were slowly thawed and stored on ice.

Electrophoretic Mobility Shift Assays. Samples of 10 μL , comprising 3 μM F17/27-0 or F17/27-4 in the experimental buffer, supplemented with 5% (v/v) glycerol, were incubated for 15 min at 20°C in the presence of 0–10.5 μM KF. Samples were then applied to 4% nondenaturing polyacrylamide minigels (Bio-Rad) and electrophoresed in 90 mM Tris-Borate (pH 8.3) for 35 min at 85 V/gel. Following electrophoresis, gels were treated with the nucleic acid specific stain SYBR Gold (Invitrogen) and imaged using an FMBIO II fluorescence scanning system (Hitachi).

Analytical Ultracentrifugation. Analytical ultracentrifugation experiments were conducted in an Optima XL-A analytical ultracentrifuge (Beckman-Coulter) using an An-Ti60 rotor and double-sector 12 mm path length cells containing quartz windows and charcoal-filled Epon centerpieces. For sedimentation velocity experiments, samples of 400 μL comprising either 3 μM F17/27-mer or 12 μM KF in the experimental buffer were centrifuged at 50 000 rpm and 20°C . At 1 min intervals, the absorbance was measured at 0.005 cm increments along the centrifuge cell. The absorption of the F17/27-mer samples was monitored at 495 nm, while that of the KF sample was monitored at 280 nm. Data were analyzed in terms of a continuous mass distribution model using SEDFIT (25).

For sedimentation equilibrium experiments, samples of 100 μL comprising 3 μM F17/27-mer and 0–10.5 μM KF in the experimental buffer were centrifuged at the desired rotor speed (11 000–28 000 rpm) at 20°C . At 4 h intervals, the 495 nm absorbance of each sample was measured at 0.001 cm increments along the centrifuge cell. The time for the attainment of equilibrium was generally 24 h, the criterion being that consecutive scans were superimposable. At equilibrium, the cells were scanned 10 times as described above and the data averaged. Samples were then centrifuged at 50 000 rpm for 3 h and scanned as described above to provide a baseline correction at each wavelength. This correction was necessary to allow for any variation in the background absorbance of the cells and was obtained by averaging the absorbance of the solute-depleted region near the sample meniscus.

The micromolar reactant concentrations used for these measurements are several orders of magnitude greater than the K_d of 7 nM for the KF•DNA complex (26). Given that the binding is at the stoichiometric limit under these conditions, no attempt was made to recover the binding constants; rather, data were analyzed in terms of a sedimenting mixture of noninteracting species. Sedimentation equilibrium gradients were analyzed using the curve fitting features of Sigmaplot version 8.0 (SPSS) according to the conservation of mass formalism

$$A_\lambda = \sum_{i=1}^j \left(\frac{A_{i,\lambda} \left\{ \exp \left[\frac{\bar{M}_i \omega^2 (r^2 - r_m^2)}{2RT} \right] \right\} \left[\frac{\bar{M}_i \omega^2 (r_b^2 - r_m^2)}{2RT} \right]}{\left\{ \exp \left[\frac{\bar{M}_i \omega^2 (r_b^2 - r_m^2)}{2RT} \right] \right\} - 1} \right) + b \quad (1)$$

where A_λ is the total loading absorbance at wavelength λ , $A_{i,\lambda}$ is the cell-average absorbance of species i at wavelength λ , \bar{M}_i is the reduced (buoyant) molar mass of species i , ω is the rotor speed (radians per second), r is the radial distance from the center of rotation (centimeters), r_m is the radial position of the sample meniscus, r_b is the radial position of the base of the centrifuge cell, R is the gas constant ($8.314 \text{ J mol}^{-1} \text{ K}^{-1}$), T is the absolute temperature (kelvin), and b is the background absorbance. The term \bar{M}_i is equivalent to $M_i(1 - \bar{v}_i\rho)$, where M_i is the molar mass of species i , \bar{v}_i is the partial specific volume of species i (milliliters per gram), and ρ is the solvent density (grams per milliliter). The partial specific volume of KF and the density of the experimental buffer solution were calculated using SEDNTERP as 0.741 mL/g and 0.999 g/mL, respectively. The partial specific volume of the 17/27-mers was assumed to be 0.550 mL/g (27). During the analysis, the values of $A_{i,\lambda}$ and \bar{M}_i were freely optimized for the best fit to eq 1.

Steady-State Fluorescence Spectroscopy. All measurements were taken at 20°C using a model 8100 spectrofluorimeter (Horiba Jobin Yvon) in the L-format (single-channel) configuration. Polarized fluorescence intensities were collected using an integration time of 2 s and represent the average of 10 consecutive readings. Raw data were corrected for fluctuations in the output of the 450 W xenon lamp by means of a quantum counter (3 g/L rhodamine B in ethylene glycol), and for background fluorescence using an appropriate reagent blank. The fluorescence anisotropy, r , was calculated using the equation

$$r = \frac{I_{VV} - GI_{VH}}{I_{VV} + 2GI_{VH}} \quad (2)$$


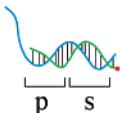

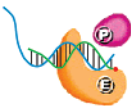
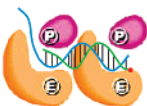
where I is the polarized fluorescence intensity and the subscripts denote the orientation, either vertical (V) or horizontal (H), of the excitation and emission polarizers, respectively. The grating correction factor G , which accounts for differential transmission of I_{VV} and I_{VH} through the emission monochromator, is given by the equation

$$G = \frac{I_{HV}}{I_{HH}} \quad (3)$$

The standard deviation associated with each anisotropy measurement was typically ± 0.002 unit.

Fluorescence Titrations and Data Analysis. Titrations of the F17/27-mers with KF were carried out in 3 mL capacity quartz cuvettes. In a typical experiment, small (2–5 μL) aliquots of KF were added to a 1.3 mL solution of 6 nM F17/27-mer in the experimental buffer. Following each addition, the cuvette was gently shaken to mix the contents, returned to the sample compartment, and left for 5 min to re-equilibrate to 20°C . The fluorescence anisotropy was determined as described above using excitation and emission wavelengths of 490 nm (4 nm) and 520 nm (4 nm), respectively, where the numbers in parentheses refer to the spectral bandpass. Data were plotted during the course of the titration, and titrations concluded once the anisotropy had stopped responding to the addition of KF.

Table 2: Fluorescence Properties of Matched Primer/Template F17/27-0 Alone and Complexed with KF

Representation ^a	Species	Designation ^b	Anisotropy (r) ^c	Enhancement factor (R) ^c
	KF	P	N/A	N/A
	F17/27-0	D	$r_D = 0.097$	$R_D = 1.000$
	F17/27-0•KF _p	DP _p	$r_{DP_p} = 0.162$	$R_{DP_p} = 1.000$
	F17/27-0•KF _s	DP _s	$r_{DP_s} = 0.216$	$R_{DP_s} = 1.860$
	F17/27-0•KF ₂	DP ₂	$r_{DP_2} = 0.335$	$R_{DP_2} = 1.860$

^a The polymerase domain of KF is colored purple and denoted by the letter P. The exonuclease domain is colored orange and denoted by the letter E. The primer and template strands are colored green and blue, respectively. The depictions serve merely as convenient representations of the KF•DNA complexes and do not purport to represent their actual organization. ^b The 1:1 complexes with KF bound at the primary or secondary sites are designated with a subscript p or s, respectively. ^c The fluorescence anisotropy parameter r_{DP} and the intensity enhancement factors R_{DP} , R_{DP_p} , R_{DP_s} , and R_{DP_2} were assigned values as described in the text. The intensity factor for DNA alone, R_D , is defined as unity. The fluorescence anisotropy parameters r_{DP_p} , r_{DP_s} , and r_{DP_2} were estimated from nonlinear least-squares analysis of the corresponding data in Figure 6 according to eq 7. These parameters were fixed in the final analysis.

constraints already described, while the values of K_p and K_s were freely optimized. The value of r_D was fixed as described above. Once physically reasonable estimates of r_{DP_p} , r_{DP_s} , and r_{DP_2} were obtained, their values were fixed (Tables 2 and 3) and the data reanalyzed to obtain best-fit estimates of K_p and K_s , together with their associated uncertainties.


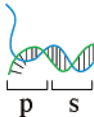

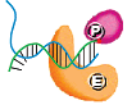

RESULTS

Description of the Experimental System. The purpose of this study is to examine the self-association of KF in the presence of DNA and the possible linkage between self-association and the primary binding mode of the enzyme. Previous time-resolved fluorescence anisotropy experiments with internally dansyl-labeled 17/27-mers have shown that while the interaction produces an equilibrium mixture of polymerizing and editing complexes, it is possible to study the polymerizing complex with minimal contamination from the editing complex using a correctly base paired primer/template (20, 21). Similarly, it is possible to study the editing complex in isolation using a primer/template containing four consecutive mismatches near the 3' end of the primer strand. Accordingly, we synthesized a series of oligonucleotides that would form primer/templates with these properties (Table 1). Since we are not concerned with active site partitioning

in this study, we have moved the probe to the 5' end of the primer strand, where it is less likely to interfere with the interaction(s) of interest. Furthermore, we have replaced the dansyl moiety with fluorescein since the latter can be detected at lower concentrations and has a visible absorption band that is well-removed from those of the protein and DNA components. It should be noted that dNTPs are absent in all experiments to prevent extension of the primer strand. Likewise, we utilized an exonuclease-deficient D424A mutant of KF (12) to prevent exonucleolytic degradation of the primer strand during the experiments.

Electrophoretic Mobility Shift Analysis of the Interaction of KF with Primer/Template DNA. The interaction between KF and the two primer/templates was examined initially using an electrophoretic mobility shift titration. The results of typical titrations performed with a constant concentration of F17/27-0 or F17/27-4 (3 μ M in both cases) and increasing concentrations of KF (0–10.5 μ M) are shown in panels A and B of Figure 1, respectively. The reagent concentrations used in these experiments were chosen to match those employed in our previous time-resolved fluorescence anisotropy studies (21). For both the matched and mismatched DNA, progressive addition of KF results in a diminution of the band representing the free primer/template and a con-

Table 3: Fluorescence Properties of Mismatched Primer/Template F17/27-4 Alone and Complexed with KF

Representation ^a	Species	Designation ^b	Anisotropy (<i>r</i>) ^c	Enhancement factor (<i>R</i>) ^c
	KF	P	N/A	N/A
	F17/27-4	X	$r_X = 0.094$	$R_X = 1.000$
	F17/27-4•KF _p	XP _p	$r_{XP_p} = 0.132$	$R_{XP_p} = 1.000$
	F17/27-4•KF _s	XP _s	$r_{XP_s} = 0.196$	$R_{XP_s} = 1.860$
	F17/27-4•KF ₂	XP ₂	$r_{XP_2} = 0.325$	$R_{XP_2} = 1.860$

^a See footnote a of Table 2. ^b See footnote b of Table 2. ^c See footnote c of Table 2.

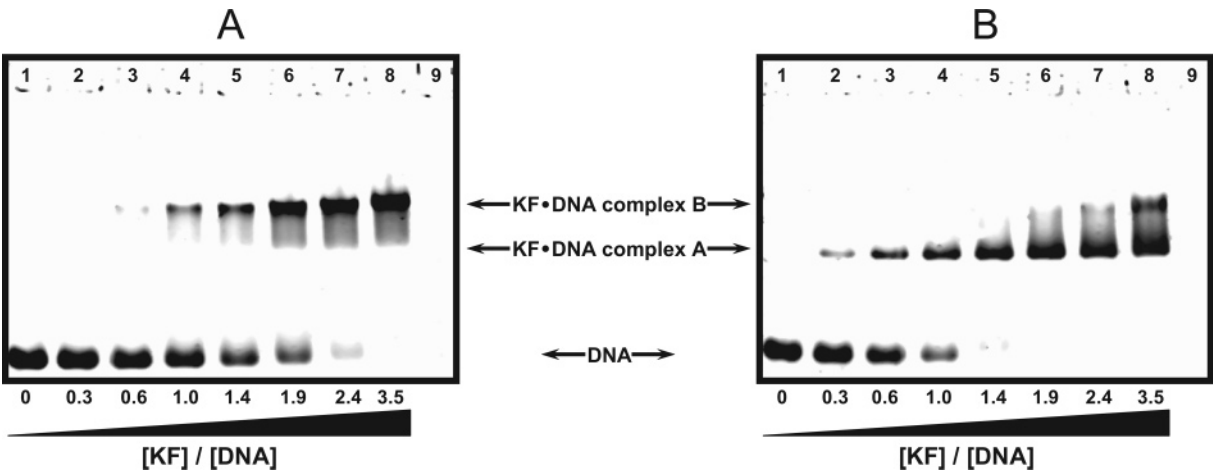


FIGURE 1: Electrophoretic analysis of the interaction of KF with DNA primer/templates. Samples were incubated for 15 min at 20 °C. (A) Titration of 3 μ M matched primer/template 17/27-0 with KF. The KF:DNA ratio is indicated under each lane. Lane 9 contained 10.5 μ M KF in the absence of DNA. The identities of the discrete bands are also indicated. (B) As for panel A, except the primer/template was the quadruply mismatched species F17/27-4.

comitant evolution of one or two bands with retarded electrophoretic mobility, reflecting the formation of KF•DNA complexes. In the case of the matched primer/template, a single retarded band (designated complex B) is observed throughout the course of the titration (Figure 1A). The mismatched primer/template also exhibits a single band throughout most of the titration, but this complex (designated complex A) migrates considerably faster than complex B (Figure 1B). Interestingly, a second band corresponding to

complex B is observed at the highest KF concentrations, suggesting that complex B contains two or more KF molecules bound to the DNA. It should be noted that for both the matched and mismatched systems, a significant degree of smearing is observed (i) between the complex A and complex B bands and (ii) ahead of the leading edge of the complex A band. This suggests that complexes A and B are both populated in the two systems but dissociate to some extent on the time scale of the assay. Nevertheless, it is

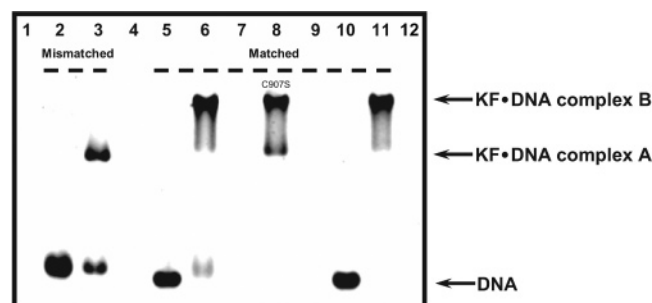


FIGURE 2: Electrophoretic mobility shift analysis of control samples. Samples were incubated for 15 min at 20 °C: lane 2, 3 μ M mismatched F17/27-4 primer/template; lane 3, 3 μ M F17/27-4 and 5.6 μ M KF; lane 4, 5.6 μ M KF; lane 5, 3 μ M matched F17/27-0 primer/template; lane 6, 3 μ M F17/27-0 and 10.5 μ M KF; lane 7, 10.5 μ M KF; lane 8, 3 μ M F17/27-0 and 10.5 μ M KF (C907S mutant); lane 9, 10.5 μ M KF (C907S mutant); lane 10, 3 μ M F17/27-0 in the presence of 1 mM DTT; lane 11, 3 μ M F17/27-0 and 10.5 μ M KF in the presence of 1 mM DTT; and lane 12, 10.5 μ M KF in the presence of 1 mM DTT. The positions of free DNA and KF•DNA complexes A and B are indicated at the right.

apparent that the slower-moving complex B is the predominant species formed with the matched primer/template, while the faster-moving complex A predominates in the case of the mismatched primer/template.

Since KF contains a single cysteine residue (Cys907), the slower-migrating complex B might arise from the binding of a disulfide-linked KF dimer to the primer/template. However, complex B was still present after KF was incubated with F17/27-0 in the presence of 1 mM DTT, which would be expected to prevent disulfide bond formation (Figure 2). Moreover, a similar gel pattern was obtained when F17/27-0 was incubated with the C907S KF mutant that is incapable of forming a disulfide bond (Figure 2). These observations indicate that complex B does not represent a disulfide-linked KF dimer.

Analytical Ultracentrifuge Analyses of the Interaction of KF with Primer/Template DNA. To ascertain the stoichiometries of the two DNA–protein complexes observed in the gel electrophoretic titrations, we carried out an analytical ultracentrifugation analysis of the individual reactants and their binary mixtures. As the first step, sedimentation velocity analysis was used to determine the molar masses of the individual reactants. Figure 3A presents a series of radial 495 nm absorbance scans of a 3 μ M sample of the F17/27-0 primer/template recorded at various times during centrifugation (increasing from left to right). The solid lines were obtained from a $c(M)$ analysis (28), the distribution for which is shown in Figure 3C. The distribution is monomodal, indicating that the sample sediments as a single species. The maximum of the distribution corresponds to a modal reduced (buoyant) molar mass of 6.3 kDa. Given a partial specific volume of 0.55 mL/g for DNA, the buoyant mass corresponds to a physical molar mass of 14.9 kDa, which is in good agreement with the value of 14.1 kDa predicted for the labeled primer/template duplex. A similar sedimentation velocity analysis of a 12 μ M KF sample recorded at 280 nm is shown in Figure 3D–F. Again, the distribution is essentially monomodal. In this case, the maximum corresponds to a modal buoyant molar mass of 17.9 kDa, which, assuming a partial specific volume of 0.74 mL/g, equates to a physical molar mass of 68.8 kDa, consistent with the value of 68.1 kDa predicted for a KF monomer. Closer inspection

of the mass distribution of the KF sample reveals that a small but perceptible proportion ($\sim 3\%$) sediments with a buoyant molar mass of ~ 35 kDa, consistent with a dimer (Figure 3F, inset). The lack of baseline resolution between the monomer and dimer peaks indicates the two species interconvert on the time scale of the experiment, suggesting that the dimer represents a bona fide equilibrium product and not a nonspecific aggregate formed simply by virtue of the high protein concentration employed (29). Thus, while KF is expected to exist essentially as a monomer, at least up to a concentration of 12 μ M, it has the capacity to dimerize in solution.

Sedimentation velocity could in principle be used to measure the stoichiometries of the KF•F17/27-mer complexes. However, this method is unlikely to yield an unequivocal outcome since the data are influenced by both the size and shape of the various sedimenting species. To overcome this potential problem, we elected to use sedimentation equilibrium. This method is as rigorous as sedimentation velocity and has an advantage in that the data are not biased by molecular shape. To further simplify the analysis, data were obtained from the 495 nm absorption of the fluorescein probe. Under these conditions, it is possible to determine the effect of KF on the apparent molar mass of the DNA. Moreover, since the protein is “invisible” at 495 nm, it is not necessary to deconvolute the data into discrete contributions from both components. Since the micromolar DNA concentrations used for optical absorbance measurements are much greater than the K_d of 7 nM for the KF•DNA complex (26), the binding is at the stoichiometric limit and no attempt was made to recover the binding constants from equilibrium centrifugation of the KF–DNA mixtures. Instead, data were analyzed in terms of sedimenting mixtures of noninteracting species, which is valid under conditions of stoichiometric binding (28).

Using sedimentation equilibrium, we monitored the distribution of 3 μ M samples of the matched and mismatched primer/templates alone and in the presence of 4.8 and 10.5 μ M KF (Figure 4). The KF concentrations were chosen on the basis of the electrophoretic data with the aim of providing distinct data sets for each system. For example, in the case of the matched primer/template, addition of 4.8 μ M KF would be expected to yield a mixture of unbound primer/template and complex B, whereas addition of 10.5 μ M KF would be expected to yield complex B exclusively. In contrast, application of the same regimen to the mismatched primer/template would be anticipated to afford complex A and an equal mixture of complexes A and B, respectively.

The equilibrium distribution of the matched primer/template F17/27-0 alone conformed to that of a single ideal solute with a buoyant molar mass of 6.6 kDa (Figure 4A), which is consistent with the value of 6.3 kDa determined by sedimentation velocity. The equilibrium distribution of 3.0 μ M F17/27-0 in the presence of 4.8 μ M KF (Figure 4C) was also fitted with a single-solute model. This provided an excellent description of the data (not shown); however, the apparent buoyant molar mass of 28.8 kDa recovered from the analysis was significantly greater than the value of 24.0 kDa expected for a 1:1 KF•DNA complex. On the basis of this observation, the gradient was reanalyzed in terms of a mixture of two solutes, allowing the buoyant molar masses

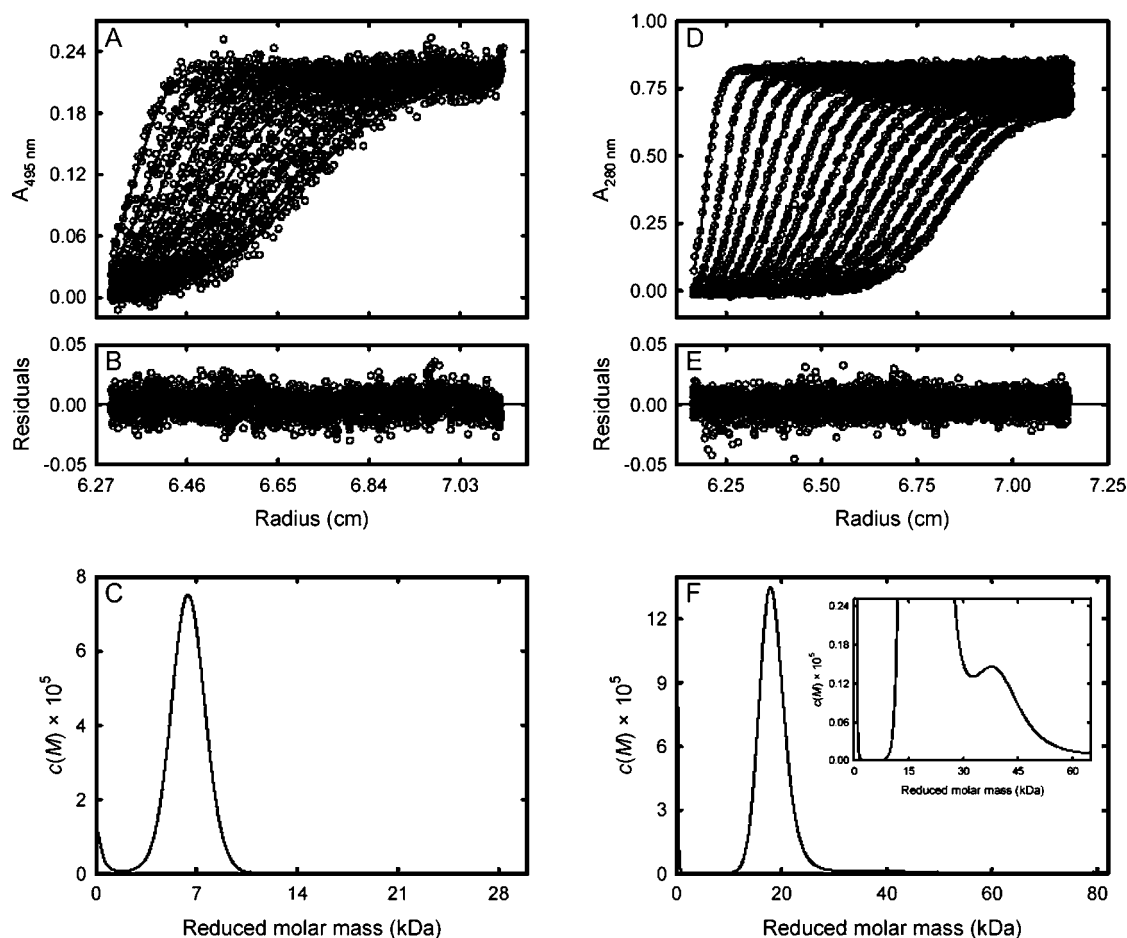


FIGURE 3: Sedimentation velocity analysis of individual DNA and protein reactants. (A) Radial time-dependent profiles of 3 μ M matched primer/template F17/27-0 measured at 495 nm (\circ). The data were analyzed in terms of a continuous mass distribution (—) using the $c(M)$ model in SEDFIT version 8.9. (B) Plot of residuals for the analysis of the experimental data in panel A. (C) Continuous mass distribution describing the experimental data in panel A. The distribution exhibits a single, well-defined maximum corresponding to a buoyant (reduced) molar mass of 6.3 kDa. (D) As for panel A, except the sample contained 12 μ M KF and the experimental data were acquired at 280 nm. (E) Plot of residuals for the analysis of the experimental data in panel D. (F) Continuous mass distribution describing the experimental data in panel D. The maximum of the distribution corresponds to a buoyant molar mass of 17.9 kDa. In the inset, the distribution has been rescaled to emphasize the presence of a minor peak corresponding to a buoyant molar mass of ca. 35 kDa.

and fractions of each species to vary for the best fit. This analysis returned buoyant molar masses of 23.9 and 40.6 kDa, which are in close agreement with the values of 24.0 and 41.7 kDa expected for 1:1 and 2:1 complexes, respectively. This result represents the first quantitative evidence that KF can form two stoichiometrically distinct complexes with primer/template DNA.

To accurately recover the fractions of each species, the analysis was repeated with the buoyant molar masses fixed to the theoretical values of the 1:1 and 2:1 complexes, while allowing the fractions to vary for the best fit. The resulting proportions of the 1:1 and 2:1 complexes were 76.3 and 23.7%, respectively. The high quality of the resulting fit is illustrated by the randomness of the plot of the residuals shown in Figure 4D. To verify the conclusions drawn above, the data in Figure 4C were reanalyzed assuming that the interaction yielded 1:1 or 2:1 KF•DNA complexes only (Figure 4C, dashed and dashed dotted lines, respectively). As anticipated, neither model could describe the data [Figure 4D (Δ and \square)].

We next examined a mixture containing a higher concentration of KF (3 μ M F17/27-0 and 10.5 μ M KF). As before, the equilibrium gradient (Figure 4E) was analyzed assuming a mixture of 1:1 and 2:1 KF•DNA complexes, allowing the

fractional populations to vary for the best fit. The resulting fit (Figure 4F) indicated that the dimeric complex was essentially the only species present (>99%). To confirm the authenticity of the 2:1 KF:DNA stoichiometry, we reanalyzed the data in Figure 4E in terms of a 2:2 KF–DNA interaction. This provided a poor description of the data (Figure 4E, dashed line) and indicates that the higher-molecular mass complex does indeed comprise two KF molecules per DNA molecule and is not the result of nonspecific aggregation of two 1:1 complexes.

The same set of sedimentation equilibrium experiments were carried out with the mismatched F17/27-4 primer/template. The primer/template alone was observed to sediment as a single species, with a buoyant molar mass of 6.0 kDa (Figure 4G,H), in good agreement with the expected value of 6.3 kDa. The equilibrium gradient of the mismatched DNA (3.0 μ M) in the presence of 4.8 μ M KF was best described by a mixture of 1:1 and 2:1 KF•DNA complexes (Figure 4I,J), with fractional populations of 79.6 and 20.4%, respectively. These results are remarkably similar to the results obtained with the matched DNA under the same conditions. Similarly, only the 2:1 complex was detected in a mixture containing 3 μ M mismatched DNA and 10.5 μ M KF (Figure 4K,L).

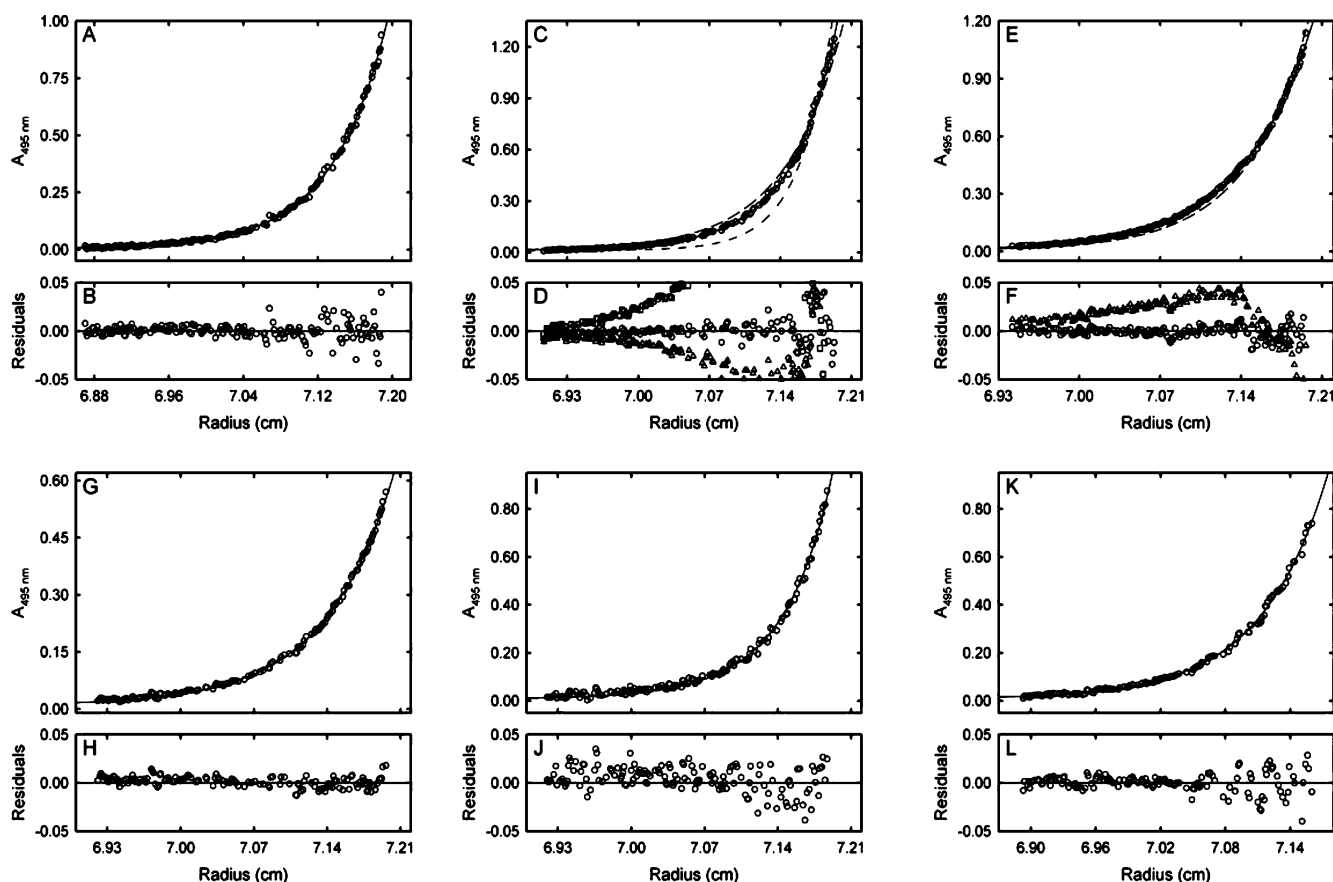


FIGURE 4: Sedimentation equilibrium analysis of the interaction of KF with matched and mismatched primer/templates. (A) Equilibrium gradient of $3 \mu\text{M}$ matched primer/template F17/27-0 centrifuged at 28 000 rpm and measured at 495 nm (\circ). The data were fitted directly to eq 1, assuming a single ideal solute at sedimentation equilibrium (—). The buoyant molar mass of the primer/template recovered from the analysis was 6.6 kDa. (B) Plot of residuals for the analysis of the experimental data in panel A. (C) As for panel A, except that the sample also contained $4.8 \mu\text{M}$ KF and was centrifuged at 15 000 rpm. The data were fitted directly to eq 1, assuming a mixture of two ideal solutes at sedimentation equilibrium (—). The buoyant molar masses of the sedimenting species were assigned values of 24.0 and 41.7 kDa, consistent with 1:1 and 2:1 KF•DNA complexes, respectively. The cell-average optical densities recovered from the analysis indicate that the proportions of primer/template engaged in the 1:1 and 2:1 complexes were 76.3 and 23.7%, respectively. The experimental data were also analyzed in terms of single ideal solutes representing the 1:1 (---) and 2:1 KF•DNA complexes (— · — · —). (D) Plot of residuals for the analysis of the experimental data in panel C. The empty circles correspond to the dual-solute model, the empty triangles to the single-solute model for the 1:1 complex, and the empty squares to the single-solute model for the 2:1 complex. (E) As for panel C, except that the sample contained $3 \mu\text{M}$ F17/27-0 and $10.5 \mu\text{M}$ KF and was centrifuged at 11 000 rpm. The solid and dashed lines correspond to the distributions predicted for homogeneous solutions of the 2:1 and 2:2 KF•DNA complexes, respectively. (F) Plot of residuals for the analysis of the experimental data in panel E. The empty circles correspond to a 2:1 complex, while the empty triangles correspond to a 2:2 complex. The 2:1 complex provides a superior fit of the experimental data. (G) As for panel A, except that the data are for the mismatched F17/27-4 primer/template. The buoyant molar mass recovered from the analysis was 6.0 kDa. (H) Plot of residuals for the analysis in panel G. (I) As for panel C, except that the data are for $3.0 \mu\text{M}$ mismatched F17/27-4 primer/template in the presence of $4.8 \mu\text{M}$ KF. The recovered fractions of the 1:1 and 2:1 complexes were 79.6 and 20.4%, respectively. (J) Plot of residuals for the analysis in panel I. (K) As for panel E, except that the data are for $3.0 \mu\text{M}$ mismatched 17/27-4 primer/template in the presence of $10.5 \mu\text{M}$ KF. The analysis indicates that the primer/template was bound exclusively (>99%) in the 2:1 complex. (L) Plot of residuals for the data in panel K.

In summary, the analytical ultracentrifugation results indicate that the retarded bands designated complex A and complex B in the electrophoretic mobility shift titrations correspond to the 1:1 and 2:1 KF•DNA complexes, respectively. The sedimentation equilibrium data are qualitatively consistent with the electrophoretic data inasmuch as KF forms both 1:1 and 2:1 complexes with primer/template DNA and that the 2:1 complex is favored at higher protein concentrations. Quantitatively, however, the two approaches appear to be at considerable odds. Specifically, sedimentation equilibrium analysis suggests that the matched and mismatched primer/templates behave identically, whereas the electrophoretic mobility shift assays indicate that the matched primer/template favors formation of the 2:1 complex and the

mismatched primer/template favors formation of the 1:1 complex.

Kinetic Stability of the KF•DNA Complexes. To reconcile the disparity between the gel electrophoretic and analytical ultracentrifugation results, the electrophoretic mobility shift assay was repeated using samples that had been incubated over the same time interval as those subjected to equilibrium centrifugation. For the sample containing $3 \mu\text{M}$ matched primer/template and $4.8 \mu\text{M}$ KF, the major species present shortly after the reagents were mixed (15 min) was the 2:1 KF•DNA complex (Figure 5A), but the proportion of this species decreased significantly once the sample had been incubated for 24 h before running the gel while the proportion of the 1:1 complex increased correspondingly (Figure 5B).

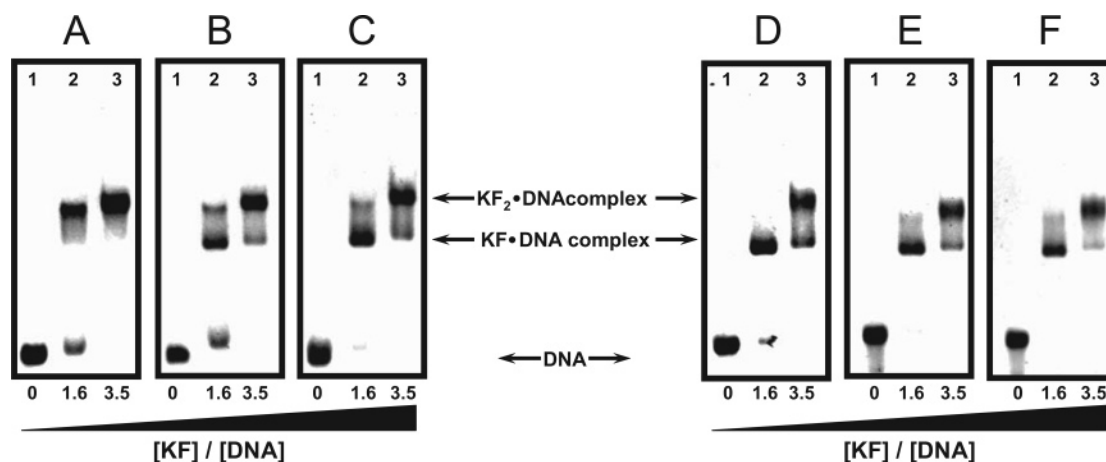


FIGURE 5: Effect of incubation time on formation of KF•DNA complexes. (A) Electrophoretic mobility shift titration of 3 μ M matched primer/template F17/27-0 with KF. The samples were incubated for 15 min prior to being loaded onto the gel. The KF:DNA molar ratio is indicated under each lane. The identities of the discrete bands are also indicated. (B and C) As for panel A, except that the samples were incubated at 20 $^{\circ}$ C for 24 and 48 h, respectively, before being loaded onto the gel. (D–F) As for panels A–C, except that the data are for the mismatched F17/27-4 primer/template.

These results indicate that the 2:1 complex formed with the matched primer/template is a metastable species that slowly dissociates to a 1:1 complex. Interestingly, the distribution of the 1:1 and 2:1 complexes after the 48 h incubation period, as judged by the intensities of the corresponding gel bands (Figure 5C), was consistent with the results of the sedimentation equilibrium analysis.

In contrast, in the case of the mismatched primer/template, the 2:1 complex appeared to slowly accumulate over time, which was particularly evident in the mixture containing 10.5 μ M KF (Figure 5D–F). Notably, the final distribution of the 1:1 and 2:1 KF•DNA complexes was similar to that observed for the matched primer/template, which is consistent with the results of the sedimentation equilibrium experiments.

These results suggest that a true equilibrium distribution of 1:1 and 2:1 complexes is not established until 24–48 h after KF is mixed with primer/template DNA. In particular, the second KF molecule appears to bind very slowly to the mismatched primer/template and to dissociate slowly from the matched primer/template. As a result of these kinetic differences, KF initially appears to form 2:1 complexes more efficiently with the matched primer/template than with the mismatched primer/template. Importantly, these results also demonstrate that the differences between the initial electrophoretic mobility shift titrations and sedimentation equilibrium measurements are not due to the methods per se, but to the fact that the electrophoretic data were collected well before the system had reached equilibrium whereas the sedimentation data were collected when the system was actually at equilibrium. When the mobility shift assay is carried out on samples that have been incubated for the same period of time as those used for sedimentation equilibrium, the gel-based data are entirely consistent with the ultracentrifugation data.

Steady-State Fluorescence Analysis of the Interaction of KF with Primer/Template DNA. In view of the surprising gel electrophoresis results, we used fluorescence anisotropy as an alternative method to probe the interaction of KF with the matched and mismatched primer/templates. Like the electrophoretic titrations, fluorescence anisotropy can provide information about the complexes present shortly after the polymerase and DNA primer/template are mixed, but the

analysis is performed in a homogeneous solution, thereby eliminating any artifacts arising from the gel matrix. In addition, it is important to confirm that the binding of a second KF molecule to DNA is not simply a consequence of the high (micromolar) protein concentrations used for the ultracentrifugation measurements. Fluorescence spectroscopy is useful for this purpose because its greater sensitivity permits detection in the more physiologically relevant nanomolar concentration range.

The matched F17/27-0 primer/template was titrated with increasing concentrations of KF, and the polarization anisotropy of the attached fluorescein probe was recorded 5 min after each addition of protein. This incubation time was similar to the initial electrophoretic mobility shift titrations described above. A typical titration profile is presented in Figure 6A. It is apparent that the addition of KF to the labeled primer/template results in an increase in the polarization anisotropy of the fluorescence emission, reflecting the slower rotational diffusion of the DNA when associated with KF. Addition of KF also causes a marked increase in the total emission intensity of the probe, suggesting that there is a direct interaction between the protein and the fluorescein probe (not shown). The data were initially analyzed using a 1:1 association model, described by eq 4 in Materials and Methods. The resulting fit was poor (Figure 6A, red line), which is particularly evident in the plot of the residuals (Figure 6B, red circles). On this basis, we extended the analysis of the fluorescence titration data to account for the binding of up to two KF molecules to a single primer/template, as described by eq 7 in Materials and Methods. During the analysis, the dissociation constants, K_p and K_s , corresponding to the first and second binding events, respectively, were optimized to fit the titration profile. This model provided a much better description of the experimental data (Figure 6A, black line, and Figure 6B, black circles). Interestingly, the K_p value of 1.6 ± 0.1 nM and the K_s value of 0.85 ± 0.07 nM recovered from the analysis are very similar. If taken on face value, this suggests that the previously defined primary and secondary sites within the matched primer/template bind KF with essentially equal affinity. However, given the function of the enzyme, it is logical that KF would bind preferentially to the primer/

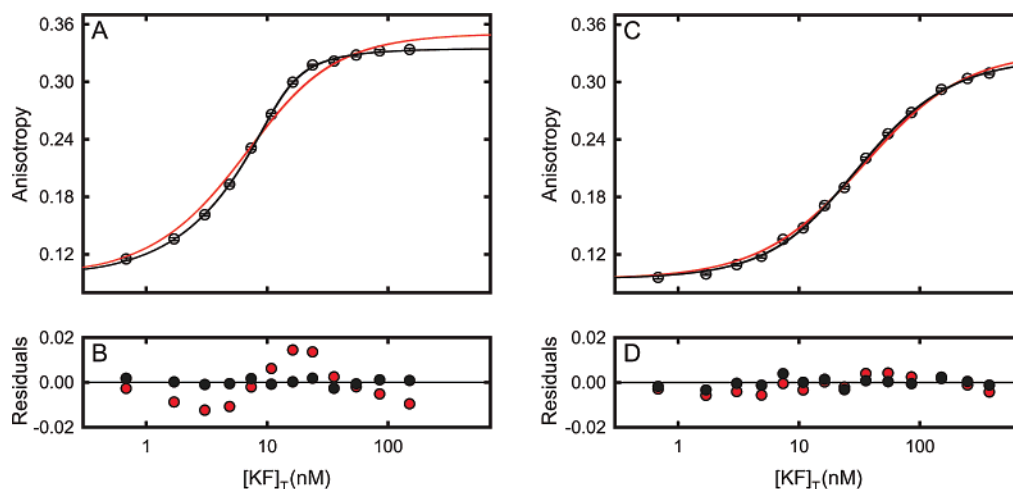


FIGURE 6: Fluorescence anisotropy titrations of primer/templates with KF. (A) Titration of 6 nM matched primer/template F17/27-0 with KF at 20 °C. The solid red line represents the best fit of the experimental data to a 1:1 binding model (eq 4), whereas the solid black line represents the best fit to a model in which the primer/template can bind up to two KF molecules (eq 7). (B) Plot of residuals for the fits shown in panel A. The residuals for the 1:1 association model are shown as solid red circles, while the residuals for the model incorporating the 1:1 and 2:1 binding modes are shown as solid black circles. (C) As for panel A, except that the data are for the mismatched F17/27-4 primer/template. (D) Plot of residuals for the fit shown in panel C.

template junction (i.e., the primary site) instead of the “blunt-ended” region upstream (the likely location of the secondary site). With this in mind, it is likely that K_s represents the unresolved product of the actual dissociation constant and a cooperativity parameter ω . Unfortunately, attempts to analyze the data in terms of cooperativity were unsuccessful due to the high degree of correlation between the recovered K_s and ω values.

An analogous fluorescence titration was carried out with the mismatched F17/27-4 primer/template (Figure 6C). Once again, a better description of the data was obtained using the model incorporating both 1:1 and 2:1 KF•DNA complexes. In this case, however, the K_p and K_s values recovered from the analysis were quite different (3.8 ± 1.7 and 51.6 ± 5.6 nM, respectively). The significantly weaker binding of the second KF molecule observed here is in qualitative agreement with the electrophoretic data in Figure 1A. It must be stressed that although the K_s value obtained in the case of the mismatched primer/template is substantially higher than the corresponding value for the matched primer/template, the actual values may be identical. In this case, the degree of cooperativity associated with the binding of the second KF molecule would simply be greater for the matched primer/template than for the mismatched primer/template, a notion entirely consistent with our experimental findings.

In strict terms, K_p and K_s are apparent rather than true dissociation constants, since the equilibrium distribution of species is established very slowly, as noted in the preceding section. Nevertheless, K_p and K_s are relevant to the KF•DNA complexes that are formed on the time scale of a polymerization or editing reaction.

In conclusion, the fluorescence titrations confirm that KF can form both 1:1 and 2:1 complexes with the primer/templates. Moreover, the results establish that the 2:1 complex is populated when the KF concentration is in the nanomolar range. Most importantly, the fluorescence titrations recapitulate the results of the initial gel electrophoretic titrations. Hence, when complexes of KF with matched or mismatched DNA primer/templates are examined shortly

after the protein and DNA are mixed, it is apparent that formation of the 2:1 complex is favored by the matched primer/template and that the 1:1 complex is favored by the mismatched primer/template, regardless of the method used to monitor the interaction.

Location of the Secondary Protein Binding Site. According to the high-resolution structures available for replicating complexes of the KF homologues from the bacterium *Thermus aquaticus* and from bacteriophage T7, the primary binding site for KF is most likely located at the junction between the duplex and single-stranded regions of the primer/template (17, 18). In principle, a second KF molecule could bind either to the single-stranded template or to the upstream duplex. To test the former possibility, we created an F17/20-mer primer/template in which the template overhang was shortened from 10 to 3 nucleotides (Table 1). The base sequence within the duplex region and the shortened template overhang was otherwise identical to F17/27-0. From cocrystal structures of homologous polymerases described above, it is evident that such a short overhang would barely exit the polymerase domain, let alone provide a binding site for a second KF molecule (17, 18). Accordingly, this modification is expected to disrupt binding of a second KF monomer if this molecule actually interacts with the template overhang. However, the gel pattern obtained when KF was incubated with the 17/20-mer primer/template was identical to that obtained with the original 17/27-mer (Figure 7). Moreover, sedimentation equilibrium experiments confirmed that KF still formed a 2:1 complex with the F17/20-0 primer/template (Figure 7D,E). On the basis of these results, it is unlikely that the second KF molecule binds to the template overhang.

It is more likely that the second KF molecule binds to the duplex upstream of the primary binding site. This location is also consistent with the results of the fluorescence anisotropy titrations. The fluorescence intensity and anisotropy parameters recovered from that analysis indicate that the local environment of the fluorescein probe was significantly altered when the secondary KF binding site was occupied (Tables 2 and 3). In particular, the quantum yield of the fluorescein probe was markedly enhanced when the second KF molecule

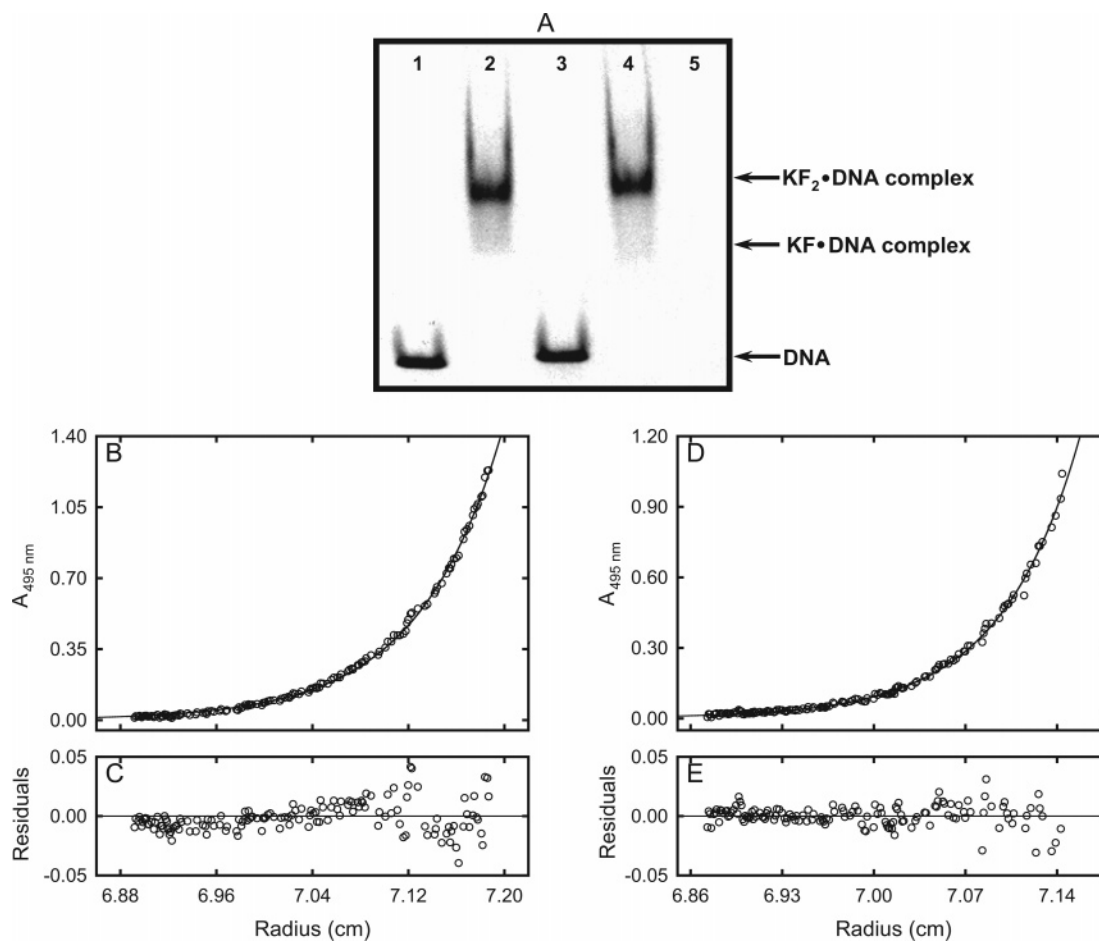


FIGURE 7: Effect of template overhang length on KF binding. Samples were incubated for 15 min at 20 °C. (A) Electrophoretic mobility shift analysis of primer/templates containing short (F17/20-0) or normal (F17/27-0) template overhangs. The duplex region of F17/20-0 is identical to that of F17/27-0, but the template overhang is reduced in length from 10 to 3 nucleotides. Lanes 1 and 2 contained 3 μ M F17/20-0 in the presence of 0 and 10.5 μ M KF, respectively. Lanes 3 and 4 contained 3 μ M F17/27-0 in the presence of 0 and 10.5 μ M KF, respectively. Lane 5 contained 10.5 μ M KF. (B) Sedimentation equilibrium data for 3 μ M F17/20-0 measured at 495 nm (\circ). The data were fitted directly to eq 1, assuming a single ideal solute at sedimentation equilibrium (—). The buoyant molar mass of the primer/template recovered from the analysis was 5.5 kDa. (C) Plot of residuals for the analysis shown in panel B. (D) Sedimentation equilibrium data for 3 μ M F17/20-0 in the presence of 10.5 μ M KF (\circ). The data were fitted directly to eq 1, assuming a single ideal solute at sedimentation equilibrium (—). The buoyant molar mass of the primer/template recovered from the analysis was 42.5 kDa, consistent with a 2:1 complex of KF with the F17/20-0 primer/template. (E) Plot of residuals for the analysis shown in panel D.

was bound and the polarization anisotropy was larger than when the primary binding site was occupied, indicating that local rotation of the probe was more restricted. Both properties indicate a direct interaction between the probe and KF. Given that the probe was attached at the 5' end of the primer strand, this interaction could certainly occur if the second KF molecule bound to the upstream duplex. It should be noted that free fluorescein does not bind to KF (29); thus, any interaction between the two arises purely by virtue of the proximity of the probe to the upstream binding site.

The location of the secondary protein binding site within the upstream duplex could potentially account for the less efficient binding of the second KF molecule to the mismatched primer/template. Previous fluorescence footprinting studies have shown that KF contacts a larger region of duplex DNA when bound in an editing complex (30). Specifically, the protein footprint is extended by 2–3 bp in the upstream direction. Hence, if the first KF monomer binds to the primer/template to form an editing complex, it may leave less space on the upstream duplex for the second KF molecule to bind. To test this possibility, we extended the upstream duplex by 5 bp, creating primer/templates F22/32-0 and F22/32-4

(Table 1). The 5 bp extension should compensate for the larger footprint of the editing complex. Interestingly, the electrophoretic mobility shift patterns obtained with F22/32-0 and F22/32-4 were essentially identical to those obtained with the original F17/27-mer primer/templates (Figure 8). Hence, the ability of a second KF molecule to bind a primer/template, either matched or mismatched, is not influenced by the length of the upstream duplex region.

DISCUSSION

KF is one of the best characterized DNA-dependent DNA polymerases. First described almost four decades ago (1), KF has since been studied by a variety of genetic (12, 31), biochemical (14, 32), kinetic (7), spectroscopic (20, 21, 26, 33, 34), and crystallographic (2, 12, 13, 16) approaches. Despite the many previous studies of this enzyme, we are aware of only two previous reports, albeit indirect, that more than one KF molecule can bind to the same DNA primer/template (35, 36). In those studies, electrophoretic gel shift titrations were performed with KF and model primer/templates (fully matched). It was noted that two discrete complexes were formed during the course of the titrations,

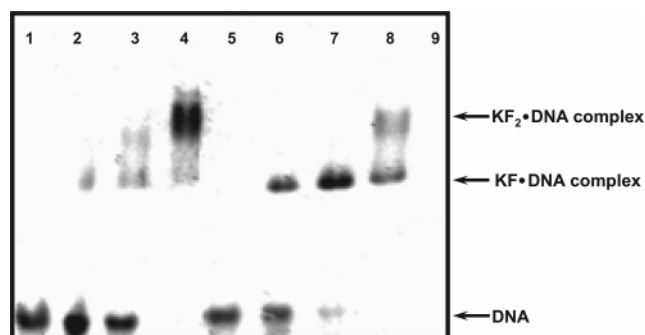


FIGURE 8: Effect of duplex length on KF–DNA interactions analyzed by the electrophoretic mobility shift assay. Samples were incubated for 15 min at 20 °C. Lanes 1–4 contained 3 μ M F22/32-0 primer/template in the presence of 0, 1.5, 3.0, and 10.5 μ M KF, respectively. Lanes 5–8 contained 3 μ M F22/32-4 primer/template in the presence of 0, 1.5, 3.0, and 10.5 μ M KF, respectively. Lane 9 contained 10.5 μ M KF.

which were assumed to represent complexes in which one or two KF molecules were bound to a single primer/template. In this study, we have obtained definitive evidence from analytical ultracentrifugation experiments that KF can indeed form both 1:1 and 2:1 complexes with primer/template DNA. A careful analysis of the sedimentation equilibrium data has established that a mixture of KF and primer/template DNA is composed of two species, with molar masses corresponding to 1:1 and 2:1 KF•DNA complexes. Alternative models based on a homogeneous 1:1 or 2:1 complex were incapable of describing the data. In addition, the steady-state fluorescence anisotropy titrations reported here reveal that KF can bind to two distinct sites within a single primer/template. Importantly, the fluorescence results show that both sites are occupied at nanomolar concentrations of KF, indicating that the 2:1 binding mode is not simply a consequence of the relatively high protein concentrations used in the analytical ultracentrifugation measurements. In fact, the dissociation constant describing the secondary KF binding site is in the 1–50 nM range for the primer/templates examined here, values that are much smaller than the micromolar dissociation constants typical of nonspecific protein•DNA complexes.

The local environmental changes reported by the fluorescein probe in the fluorescence titrations strongly suggest that the secondary KF binding site is located within the duplex region of the primer/template, upstream from the primary site at the primer 3' terminus. This was further confirmed using primer/templates in which the template overhang was shortened from 10 to 3 nucleotides, a modification that had no effect on the 2:1 KF•DNA complex. A logical question arising from these findings is whether the two bound KF monomers exist as separate entities or as a dimer. While it is formally possible that the monomers bind in isolation, two lines of evidence suggest that they actually contact one another. First, since KF can dimerize in the absence of DNA, albeit weakly (Figure 3F), it is not unreasonable to suppose that the presence of a DNA scaffold facilitates this process. Second, binding of KF to the secondary site is more than likely a cooperative phenomenon, especially in the case of the matched primer/template (Figure 5A). Cooperativity, arising from protein oligomerization on the DNA lattice, is a common theme in the context of protein–DNA interactions.

The fluorescence anisotropy and gel electrophoretic titrations suggest that the DNA-mediated dimerization of KF is linked to the primary binding mode of the enzyme. Hence, when the first KF molecule binds in the polymerizing mode, which occurs with the matched primer/template, the second KF molecule appears to bind with a significant degree of cooperativity, favoring formation of the 2:1 complex. In contrast, when the first KF molecule binds in the editing mode, as enforced by the presence of multiple mismatches within the primer/template, the second KF molecule binds with little or no apparent cooperativity. Under these conditions, the 1:1 KF•DNA complex is favored. These observations can be rationalized if the dimerization is mediated by contacts between the exonuclease domains of adjacent KF monomers. In this scenario, the dimer interface would be partially or fully occluded if the exo site of the first KF monomer was occupied by DNA. Unfortunately, this model cannot be verified directly, because there are no structural data available for the dimeric KF•DNA complex. However, structures of monomeric complexes of KF with DNA bound at the exo site have been determined (16), and structures of KF homologues containing DNA at the pol site are also available (17, 18). These structures reveal that different protein domains are used to bind the 3'-terminal region of the DNA primer strand in each case, supporting the idea that the dimerization interface overlaps with just one of the DNA-binding surfaces.

Interestingly, the linkage between KF dimerization and the primary binding mode of the enzyme appears to be a kinetic rather than true equilibrium phenomenon. The strong preference of KF to dimerize on the fully base paired rather than the mismatched primer/template is consistently observed when the complexes are monitored shortly after the enzyme and DNA are mixed, using either gel electrophoretic or fluorescence methods, as already noted. However, this preference is not apparent once the complexes have been allowed to reach equilibrium in the analytical ultracentrifuge or are simply incubated for extended periods of time prior to gel electrophoretic analysis. Under these conditions, the 2:1 KF•DNA complex is formed in roughly equal amounts with either the matched or mismatched primer/templates. Our results further indicate that the long time required to establish an equilibrium distribution of complexes is due to the slow dissociation of 2:1 complexes from the fully base paired primer/template and the slow formation of these complexes with the mismatched primer/template. The underlying reasons for these pronounced kinetic differences are not known at present, but by their very nature suggest that DNA-mediated self-association of KF may fulfill an important biological function.

The linkage between the primary mode of DNA binding and the association state of KF, although not relevant under equilibrium conditions, is likely to apply on the time scale of a polymerization or editing reaction. Hence, our results suggest that KF will be bound to a DNA primer/template as a dimer during DNA polymerization. There is a significant body of evidence indicating that replicative DNA polymerases from T4 bacteriophage (37), T7 bacteriophage (38, 39), and *E. coli* (40, 41) also function as dimers during DNA synthesis. For these systems, polymerase dimerization at a replication fork provides a mechanism for coordinating leading and lagging strand synthesis during chromosomal

replication (38–40). However, KF is derived from *E. coli* DNA polymerase I (pol I), which is involved in gap filling DNA repair rather than chromosomal replication. Moreover, in the T4 replication system, the second polymerase molecule is bound to the single-stranded DNA template (37), whereas our results indicate that the second KF molecule is bound to the upstream duplex. Hence, dimerization of KF (and by extension pol I) might serve a different functional role. For example, the second KF monomer might help to tether the primary polymerase molecule to the primer/template, thereby enhancing the processivity of the enzyme during DNA polymerization. It is also possible that DNA-mediated self-association of KF is a vestigial activity of the polymerase I enzyme that was important before the evolution of the more sophisticated prokaryotic replication machinery represented by the pol III system.

Our results also raise the intriguing possibility that an editing reaction of KF with a mismatched primer/template occurs in the context of a monomeric enzyme–DNA complex. Although dissociation of the dimeric complex from a properly base paired primer/template appears to be slow, the presence of a terminal mismatch might accelerate dissociation. The change in the association state of KF could have profound functional consequences, especially if the monomeric complex is more active in exonucleolysis than the dimeric complex. This situation could arise if protein–protein contacts somehow block the exonuclease active site in the dimeric complex. This is consistent with the idea, proposed above, that the dimerization interface and DNA-binding surface within the exonuclease domain are overlapping.

The linkage between dimerization and the primary DNA binding mode of KF is a novel finding that has not been reported before, despite almost four decades of research on this very well studied enzyme. This discovery raises important questions about the enzymatic and structural properties of the monomeric and dimeric complexes, which are the subject of ongoing research.

REFERENCES

- Brutlag, D., Atkinson, M. R., Setlow, P., and Kornberg, A. (1969) An active fragment of DNA polymerase produced by proteolytic cleavage, *Biochem. Biophys. Res. Commun.* 37, 982–989.
- Ollis, D. L., Brick, P., Hamlin, R., Xuong, N. G., and Steitz, T. A. (1985) Structure of large fragment of *Escherichia coli* DNA polymerase I complexed with dTMP, *Nature* 313, 762–766.
- Wang, J., Sattar, A. K. M. A., Wang, C. C., Karam, J. D., Konigsberg, W. H., and Steitz, T. A. (1997) Crystal structure of a pol α family replication DNA polymerase from bacteriophage RB69, *Cell* 89, 1087–1099.
- Sawaya, M. R., Pelletier, H., Kumar, A., Wilson, S. H., and Kraut, J. (1994) Crystal structure of rat DNA polymerase β : Evidence for a common polymerase mechanism, *Science* 264, 1930–1935.
- Trincao, J., Johnson, R. E., Escalante, C. R., Prakash, S., Prakash, L., and Aggarwal, A. K. (2001) Structure of the catalytic core of *S. cerevisiae* DNA polymerase η : Implications for translesion DNA synthesis, *Mol. Cell* 8, 417–426.
- Zhou, B.-L., Pata, J. D., and Steitz, T. A. (2001) Crystal structure of a DinB lesion bypass DNA polymerase catalytic fragment reveals a classic polymerase catalytic domain, *Mol. Cell* 8, 427–437.
- Kuchta, R. D., Benkovic, P., and Benkovic, S. J. (1988) Kinetic mechanism whereby DNA polymerase I (Klenow) replicates DNA with high fidelity, *Biochemistry* 27, 6716–6725.
- Capson, T. L., Peliska, J. A., Kaboord, B. F., Frey, M. W., Lively, C., Dahlberg, M., and Benkovic, S. J. (1992) Kinetic characterization of the polymerase and exonuclease activities of the gene 43 protein of bacteriophage T4, *Biochemistry* 31, 10984–10994.
- Ahn, J., Werneburg, B. G., and Tsai, M. D. (1997) DNA polymerase β : Structure-fidelity relationship from pre-steady-state kinetic analyses of all possible correct and incorrect base pairs for wild type and R283A mutant, *Biochemistry* 36, 1100–1107.
- Washington, M. T., Prakash, L., and Prakash, S. (2001) Yeast DNA polymerase η utilizes an induced-fit mechanism for nucleotide incorporation, *Cell* 107, 917–927.
- Fiala, K. A., and Suo, Z. (2004) Mechanism of DNA polymerization catalyzed by *Sulfolobus solfataricus* P2 DNA polymerase IV, *Biochemistry* 43, 2116–2125.
- Derbyshire, V., Freemont, P. S., Sanderson, M. R., Beese, L., Friedman, J. M., Joyce, C. M., and Steitz, T. A. (1998) Genetic and crystallographic studies of the 3',5'-exonucleolytic site of DNA polymerase I, *Science* 240, 199–201.
- Beese, L. S., Friedman, J., and Steitz, T. A. (1993) Crystal structures of the Klenow fragment of DNA polymerase I complexed with deoxynucleoside triphosphate and pyrophosphate, *Biochemistry* 32, 14095–14101.
- Cowart, M., Gibson, K. J., Allen, D. J., and Benkovic, S. J. (1989) DNA substrate requirements for exonuclease and polymerase activities of prokaryotic and phage DNA polymerases, *Biochemistry* 28, 1975–1983.
- Ruscitti, T., Polayes, D. A., Karu, A. E., and Linn, S. (1992) Selective immunoneutralization of the multiple activities of *Escherichia coli* DNA polymerase I supports the model for separate active sites and indicates a complex 5' to 3' exonuclease, *J. Biol. Chem.* 267, 16806–16811.
- Freemont, P. S., Friedman, J. M., Beese, L. S., Sanderson, M. R., and Steitz, T. A. (1998) Cocystal structure of an editing complex of Klenow fragment with DNA, *Proc. Natl. Acad. Sci. U.S.A.* 85, 8924–8928.
- Li, Y., Korolev, S., and Waksman, G. (1998) Crystal structures of open and closed forms of binary and ternary complexes of the large fragment of *Thermus aquaticus* DNA polymerase I: Structural basis for nucleotide incorporation, *EMBO J.* 17, 7514–7525.
- Doublie, S., Tabor, S., Long, A. M., Richardson, C. C., and Ellenberger, T. (1998) Crystal structure of bacteriophage T7 replication complex at 2.2 Å resolution, *Nature* 391, 251–258.
- Beese, L. S., Derbyshire, V., and Steitz, T. A. (1993) Structure of DNA polymerase I Klenow fragment bound to duplex DNA, *Science* 260, 352–355.
- Carver, T. E., Hochstrasser, R. A., and Millar, D. P. (1994) Proofreading DNA: Recognition of aberrant DNA termini by the Klenow fragment of DNA polymerase I, *Proc. Natl. Acad. Sci. U.S.A.* 91, 10670–10674.
- Bailey, M. F., Thompson, E. H. Z., and Millar, D. P. (2001) Probing DNA polymerase fidelity mechanisms using time-resolved fluorescence anisotropy, *Methods* 25, 62–77.
- Eis, P. E., and Millar, D. P. (1993) Conformational distributions of a four-way DNA junction revealed by time-resolved fluorescence resonance energy transfer, *Biochemistry* 32, 13852–13860.
- Warshaw, M. M., and Cantor, C. R. (1970) Oligonucleotide interactions. IV. Conformational differences between deoxy- and ribonucleoside phosphates, *Biopolymers* 9, 1079–1103.
- Joyce, C. M., and Derbyshire, V. (1995) Purification of *E. coli* DNA polymerase I and Klenow fragment, *Methods Enzymol.* 262, 3–13.
- Schuck, P. (1998) Sedimentation analysis of noninteracting and self-associating solutes using numerical solutions to the Lamm equation, *Biophys. J.* 75, 1503–1512.
- Allen, D. J., Darke, P. L., and Benkovic, S. J. (1989) Fluorescent oligonucleotides and deoxynucleotide triphosphates: Preparation and their interaction with the large (Klenow) fragment of *Escherichia coli* DNA polymerase I, *Biochemistry* 28, 4601–4607.
- Laue, T. M., Sear, D. F., Eaton, S., and Ross, J. B. A. (1993) 5-Hydroxytryptophan as a new intrinsic probe for investigating protein-DNA interactions by analytical ultracentrifugation. Study of the effect of DNA on the self-assembly of the λ cI repressor, *Biochemistry* 32, 2469–2472.
- Schuck, P. (2003) On the analysis of protein self-association by sedimentation velocity analytical ultracentrifugation, *Anal. Biochem.* 320, 104–124.
- Howlett, G. J., Minton, A. P., and Rivas, G. (2006) Analytical ultracentrifugation studies of protein associations and assembly, *Curr. Opin. Chem. Biol.* 10, 430–436.

30. Bailey, M. F., Van der Schans, E. J. C., and Millar, D. P. (2004) Thermodynamic dissection of the polymerizing and editing modes of a DNA polymerase, *J. Mol. Biol.* 336, 673–693.
31. Guest, C. R., Hochstrasser, R. A., Dupuy, C. G., Allen, D. J., Benkovic, S. J. and Millar, D. P. (1991) Interaction of DNA with DNA polymerase I studied by time-resolved fluorescence spectroscopy, *Biochemistry* 30, 8759–8770.
32. Derbyshire, V., Grindley, N. D. F., and Joyce, C. M. (1991) The 3'-5' exonuclease of DNA polymerase I of *Escherichia coli*: Contribution of each amino acid at the active site to the reaction, *EMBO J.* 10, 17–24.
33. Catalano, C. E., Allen, D. J., and Benkovic, S. J. (1990) Interaction of *Escherichia coli* DNA polymerase I with azidoDNA and dfluorescent DNA probes: Identification of protein-DNA contacts, *Biochemistry* 29, 3612–3621.
34. Hochstrasser, R. A., Carver, T. E., Sowers, L. C., and Millar, D. P. (1994) Melting of a DNA helix terminus within the active site of a DNA polymerase, *Biochemistry* 33, 11971–11979.
35. Purohit, V., Grindley, N. D. F., and Joyce, C. M. (2003) Use of 2-aminopurine fluorescence to examine conformational changes during nucleotide incorporation by DNA polymerase I (Klenow fragment), *Biochemistry* 42, 10200–10211.
36. Astatke, M., Grindley, N. D. F., and Joyce, C. M. (1995) Deoxynucleoside triphosphate and pyrophosphate binding sites in the catalytically competent ternary complex for the polymerase reaction catalyzed by DNA polymerase I (Klenow fragment), *J. Biol. Chem.* 270, 1945–1954.
37. Rechkoblit, O., Amin, S., and Geacintov, N. E. (1999) Primer length dependence of binding of DNA polymerase I Klenow fragment to template-primer complexes containing site-specific bulky lesions, *Biochemistry* 38, 11834–11843.
38. Munn, M. M., and Alberts, B. M. (1991) DNA footprinting studies of the complex formed by the T4 DNA polymerase holoenzyme at a primer-template junction, *J. Biol. Chem.* 266, 20034–20044.
39. Debsyer, Z., Tabor, S., and Richardson, C. C. (1994) Coordination of leading and lagging strand synthesis at the replication fork of bacteriophage T7, *Cell* 77, 157–166.
40. Lee, J., Chastain, P. D., Kusakabe, T., Griffith, J., and Richardson, C. C. (1998) Coordinated leading and lagging strand synthesis on a minicircular template, *Mol. Cell* 1, 1001–1010.
41. Kim, S., Dallmann, H. G., McHenry, C. S., and Marians, K. J. (1996) τ couples the leading- and lagging-strand polymerases at the *Escherichia coli* replication fork, *J. Biol. Chem.* 271, 21406–21412.
42. Marians, K. J., Hiasa, H., Kim, D. R., and McHenry, C. S. (1998) Role of the core DNA polymerase III subunits at the replication fork. α is the only subunit required for processive replication, *J. Biol. Chem.* 273, 2452–2457.

BI6024148